Emission line regions in active galaxies:

Selected studies in spectral line variability in the era of JWST and LSST

Scan for references

SWAYAMTRUPTA PANDA [1,2,3]

[1] LABORATÓRIO NACIONAL DE ASTROFÍSICA, ITAJUBÁ, BRAZIL

[2] Support Scientist, GEMINI and SOAR Observatories

[3] CNPq Fellow

spanda@lna.br

Rubin Observatory

S-PLUS

CNPq

LNA LABORATÓRIO NACIONAL DE ASTROFÍSICA UNIDADE DE PESQUISA DO MCTI

Paola Marziani (INAF-Padova), **Bożena Czerny** and the CFT-Warsaw group, **Alberto Rodriguez-Ardila** and LNA-Brazil group, **Francisco Pozo-Nuñez** (HITS-Heidelberg), **SER-SAG** team

14th Serbian Conference on Spectral Line Shapes in Astrophysics, Bajina Bašta, Serbia, June 19 - 23, 2023

Maunakea Spectroscopic Explorer

TABLE OF CONTENTS

AGN Spectral Energy Distribution, Variability, Black Hole Masses → AGNs as **Standardizable Candles**

Broad-band energy distribution in AGN

Constructing state-of-the-art AGN SEDs

Jin et al. (2017)

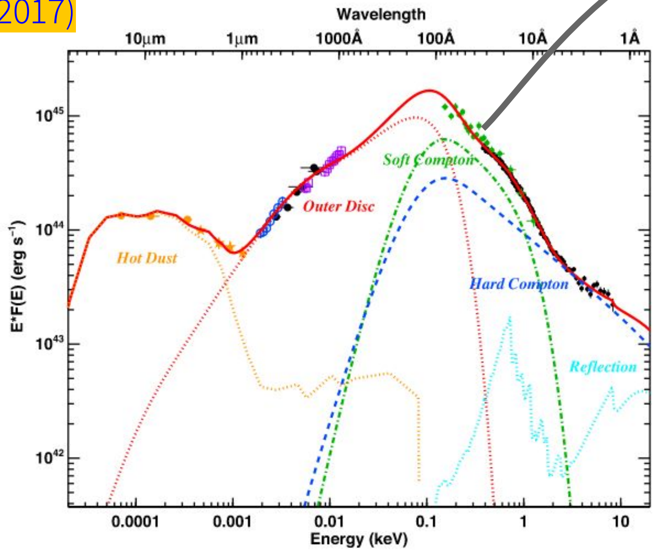

Figure 4. The broad-band SED of RX J0439.6-5311, assuming an inclination angle of 30°. The data consist of *XMM–Newton* EPIC-pn spectrum and OM photometric points (black), a combined *ROSAT* spectrum (green points in the X-ray, scaled up by 3 per cent), continual points from the *HST* COS spectra (magenta in the optical/UV, scaled down by 23 per cent), the optical spectrum from Grupe et al. (2004) (blue, scaled down by 20 per cent), and the IR photometric points including *WISE* Band 1-4 (orange circles, scaled down by 23 per cent) and 2MASS *J, H, K* (orange stars, scaled down by 23 per cent). Red solid curve is the best-fitting SED model, comprising an accretion disc component (red dotted curve), a soft X-ray Comptonization component (green dash–dotted curve), a hard X-ray Comptonization component (blue dash curve), a weak reflection component (cyan dotted curve) and a hot dust component (orange dotted curve). Note that this broad-band SED model does not consider any energy loss due to the disc wind or advection.

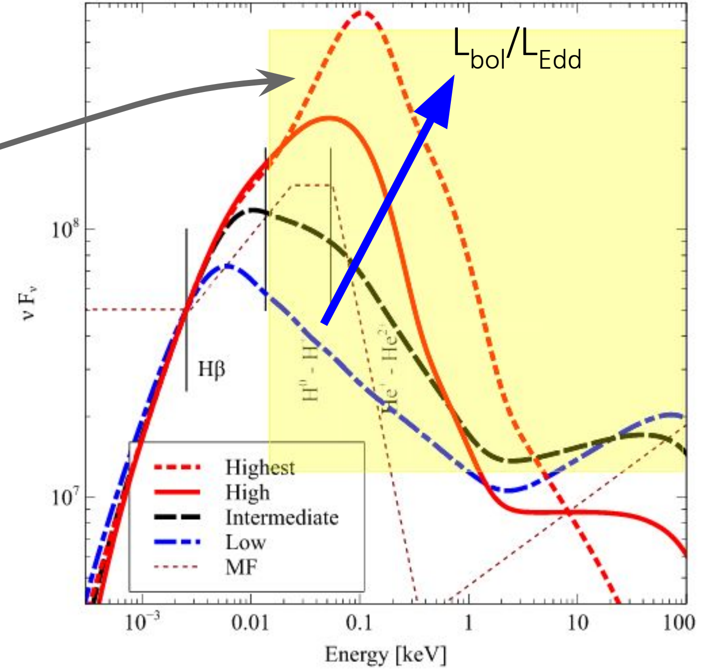

Figure 1. The four SEDs studied in this paper are compared. They are normalized to have the same intensity at the wavelength of H β, to facilitate comparison with line equivalent widths. The yellow region marks the hydrogen-ionizing part of the SED. The equivalent width of a recombination line such as H I H β is proportional to the ionizing photon luminosity within the yellow region. The energy to fully ionize He and produce He II emission is also marked. The dotted line marked 'MF' is the mean SED deduced by Mathews & Ferland (1987).

Ferland et al. (2020)

01

ACCRETION DISK (AD) AND BROAD LINE REGION (BLR)

Accretion disk structure evolution

BLR time-lag recovery

AD continuum modelling

Classifying the diversity in Type-1 AGNs using the Main Sequence of Quasars

An analogous scheme to the Hertzsprung-Russell diagram

Panda, Marziani & Czerny (2019)

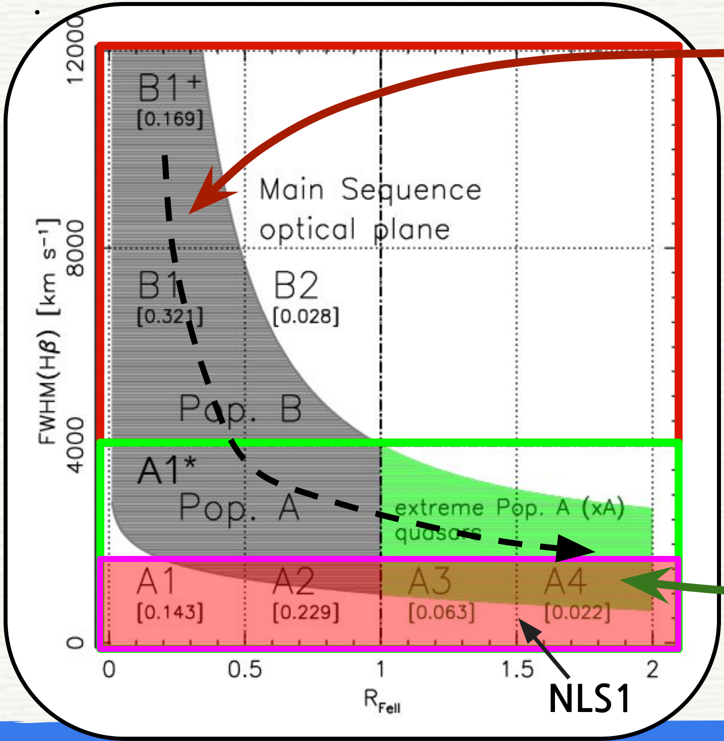

Getting closer to a global picture of AGN emission

Prominent "funnel" in slim disks for high accreting sources

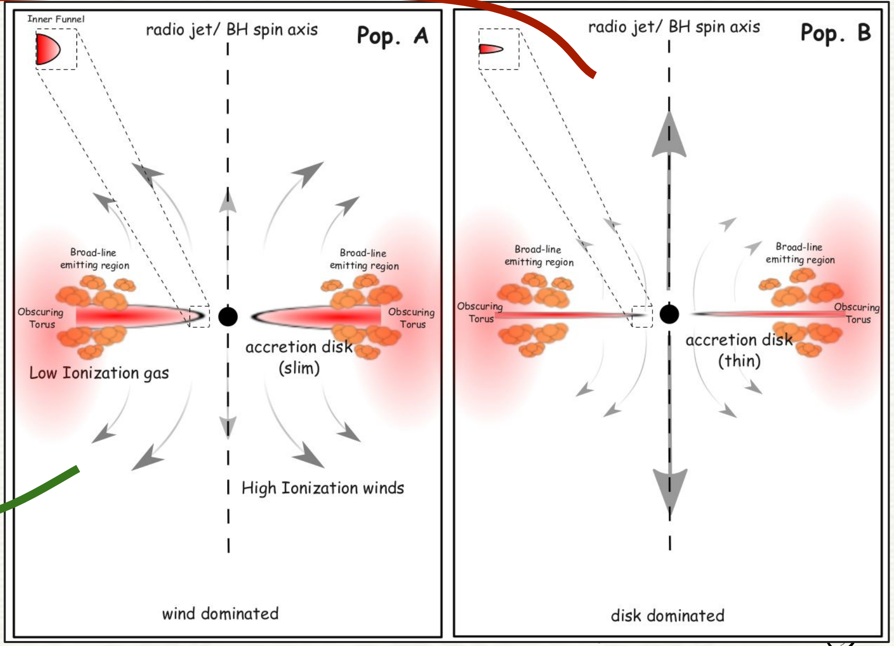

Panda (2021)

Prominent "funnel" in slim disks

Panda & Marziani (2023)

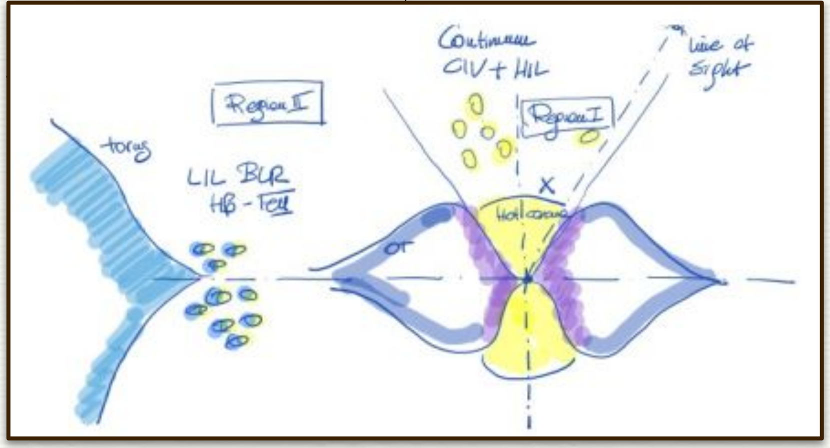

Higher accretion rates → transition to slim disks

Wang et al. (2014)

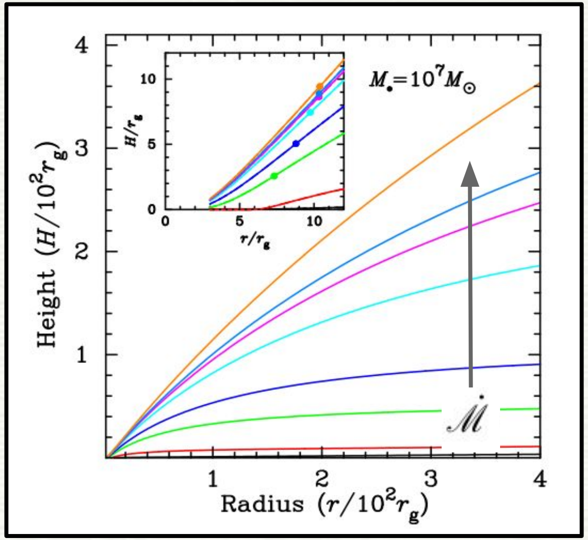

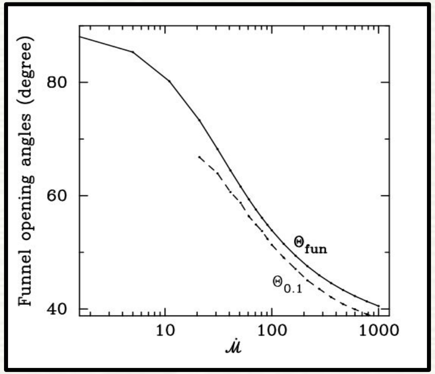

$$\dot{\mathscr{M}} = 20.1\left(\frac{\ell_{44}}{\cos i}\right)^{3/2} m_7^{-2}$$

Abramowicz et al. 1988, Wang et al. 1999, Sądowski 2011

Assimilating the slim accretion disk SEDs with X-ray corona

after fitting with observed SEDs of high accretors

10°

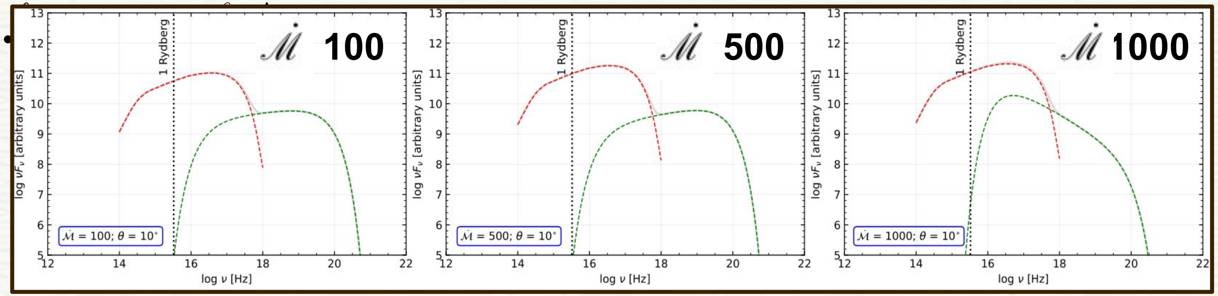

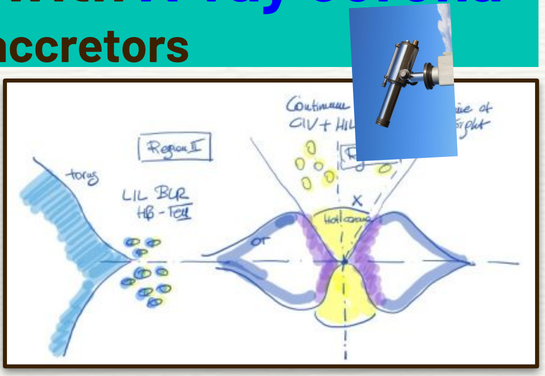

Global picture of AGN emission at high accretion rates, Photoionization modelling with CLOUDY

Stay tuned of some really interesting results and SED database!

Panda & Marziani (2023)

Assimilating the slim accretion disk SEDs with X-ray corona

after fitting with observed SEDs of high accretors

10°

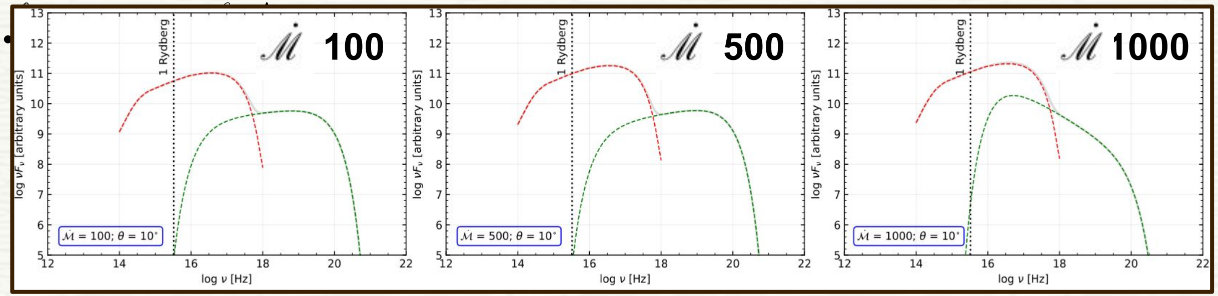

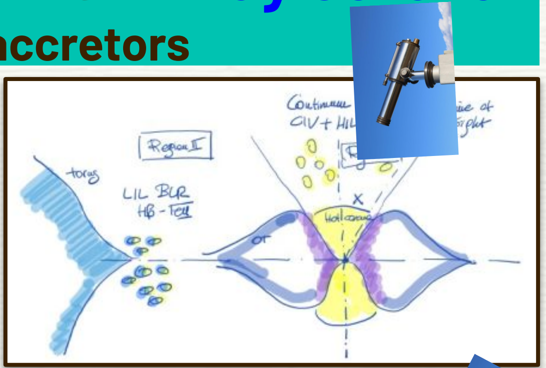

40°

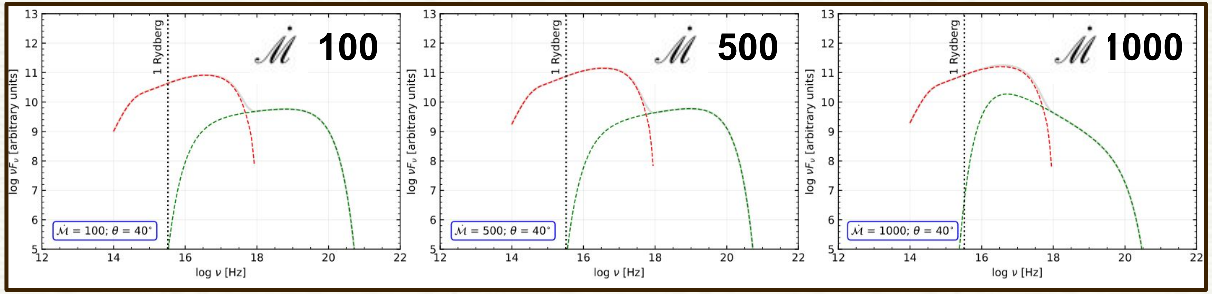

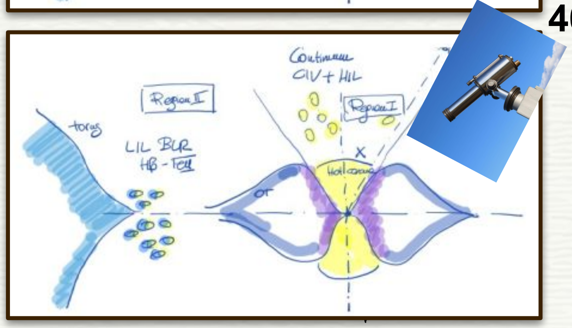

Panda & Marziani (2023)

Assimilating the slim accretion disk SEDs with X-ray corona

after fitting with observed SEDs of high accretors

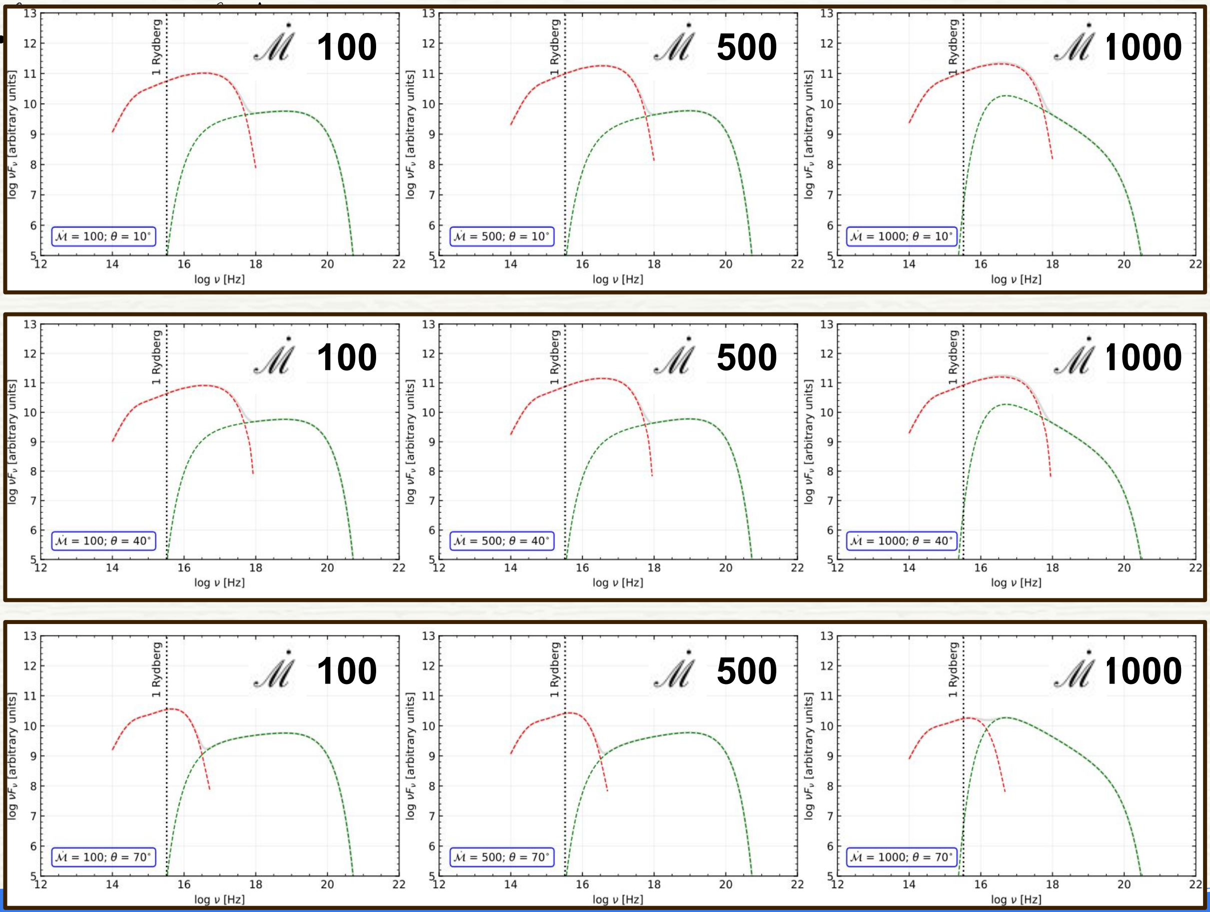

10°

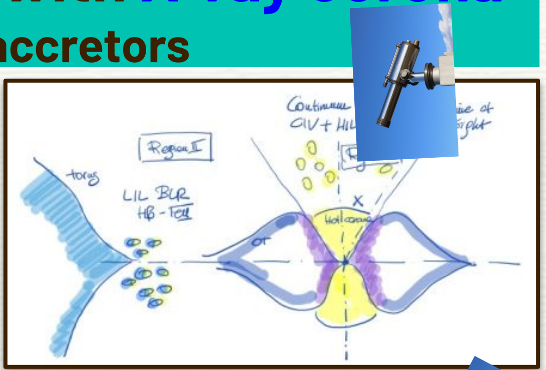

40°

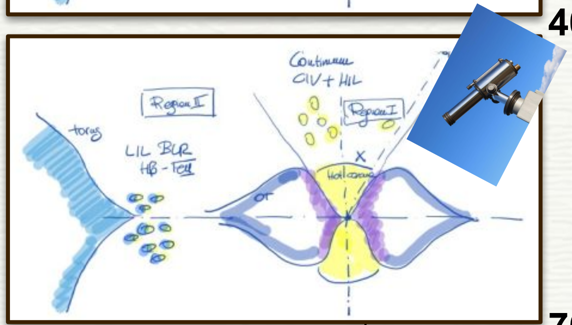

70°

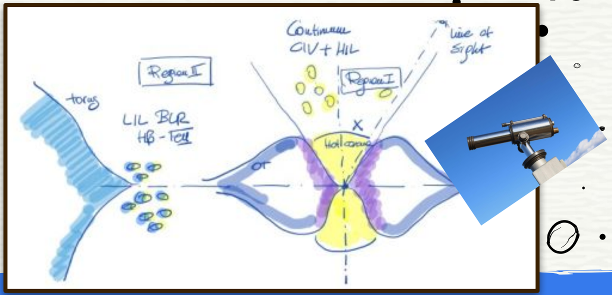

Panda & Marziani (2023)

High accreting sources with shorter BLR time-lags → deviates from the classical R-L relation

Panda (2021)

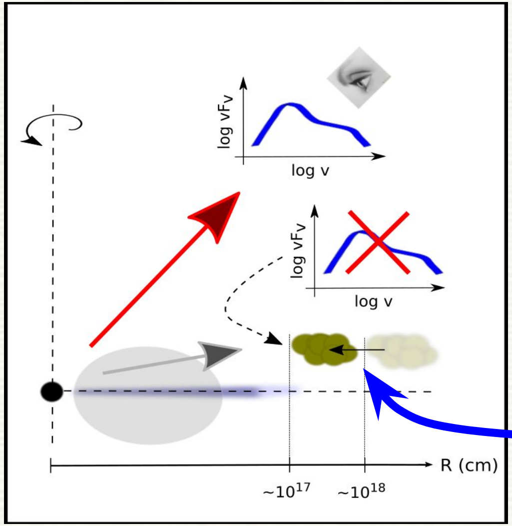

Huang et al. (2019)

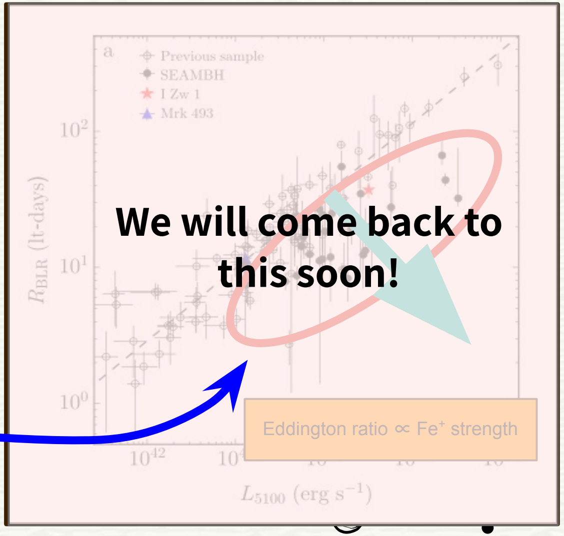

Reconcile by correcting for Fe^{+} strength (Du & Wang 2019; Panda 2022)

SOME PHYSICS

Reverberation Mapping

Given a velocity and a distance, we can use Kepler's laws to tell us the BH mass!

$$M_{\rm BH} = f\,\frac{r_{\rm BLR}{\rm FWHM}^2}{G}$$

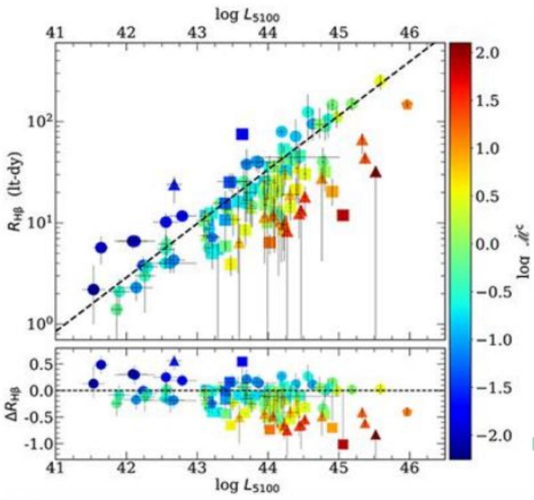

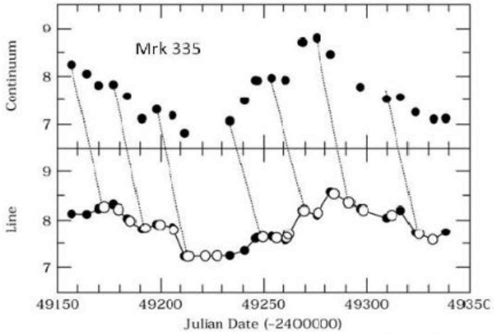

Peterson et al. (2001)

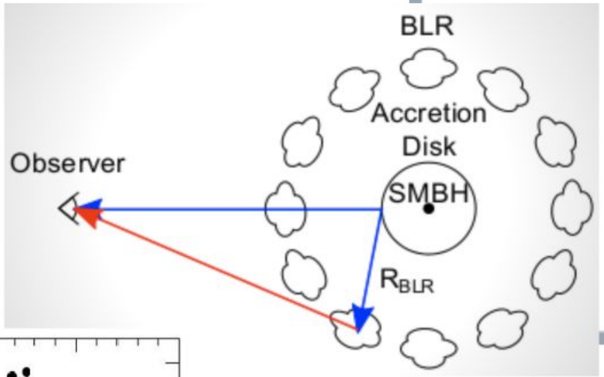

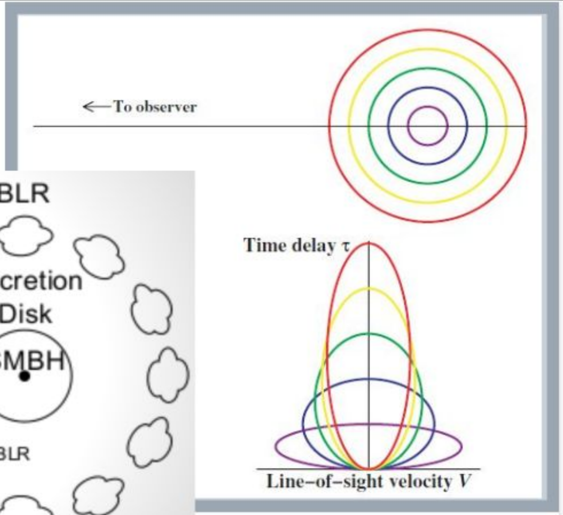

Reverberation mapping relies on the fact that the light emitted by the BLR is reprocessed from the central continuum source, and that the central continuum source is variable

We have ~200 RM AGNs now with Hβ-emitting BLR sizes!

The Vera C. Rubin Observatory

The goal of the Vera C. Rubin Observatory project is to conduct the **10-year Legacy Survey of Space and Time (LSST)**. LSST will deliver a 500 petabyte set of images and data products - create a decade-long movie of our Universe, that will address some of the most pressing questions about the structure and evolution of the universe accounting for tens of millions of AGNs (z ≳ 7).

The 8.4-meter Simonyi Survey Telescope uses a special three-mirror design, which creates an exceptionally wide field of view, and has the ability to **survey the entire sky in only three nights**.

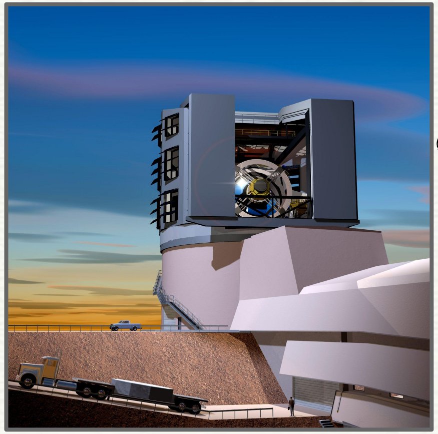

Panda et al. (2019)

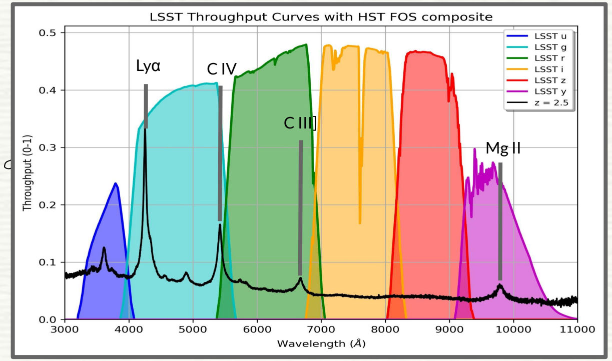

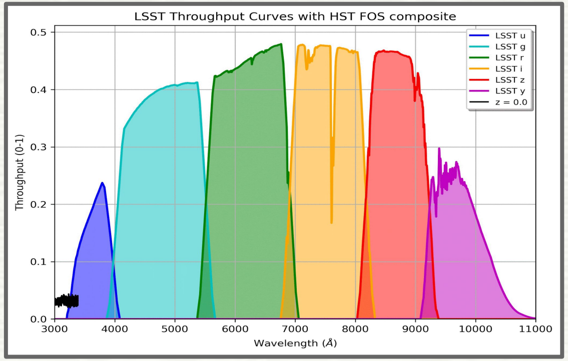

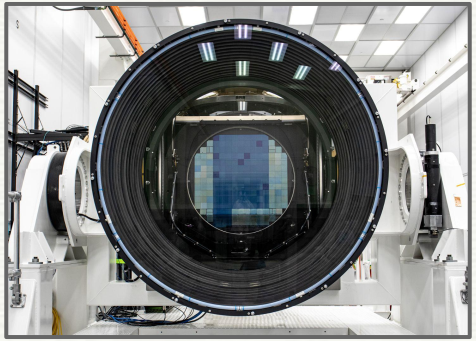

3200 Megapixel camera

Photo-RM with VRO-LSST

Representative light-curves from OpSim runs (DDF)

Panda et al. 2019

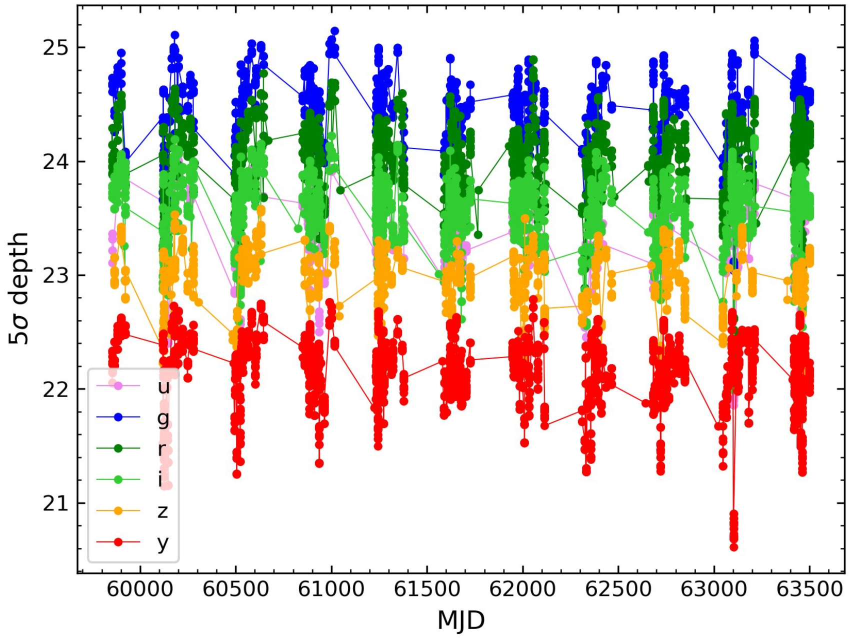

OpSim Run:
ddf_dither0.00_v1.7_10yrs

ELAIS-S1 field
RA=00:37:48, Dec=-44:01:30

# of visits in 10 years:

u → 1056
g → 2239
r → 4495
i → 4496
z → 2230
y → 4436

Czerny, Panda, et al. (2023)

Predictions for LSST: BLR time-lag vs. AGN luminosity

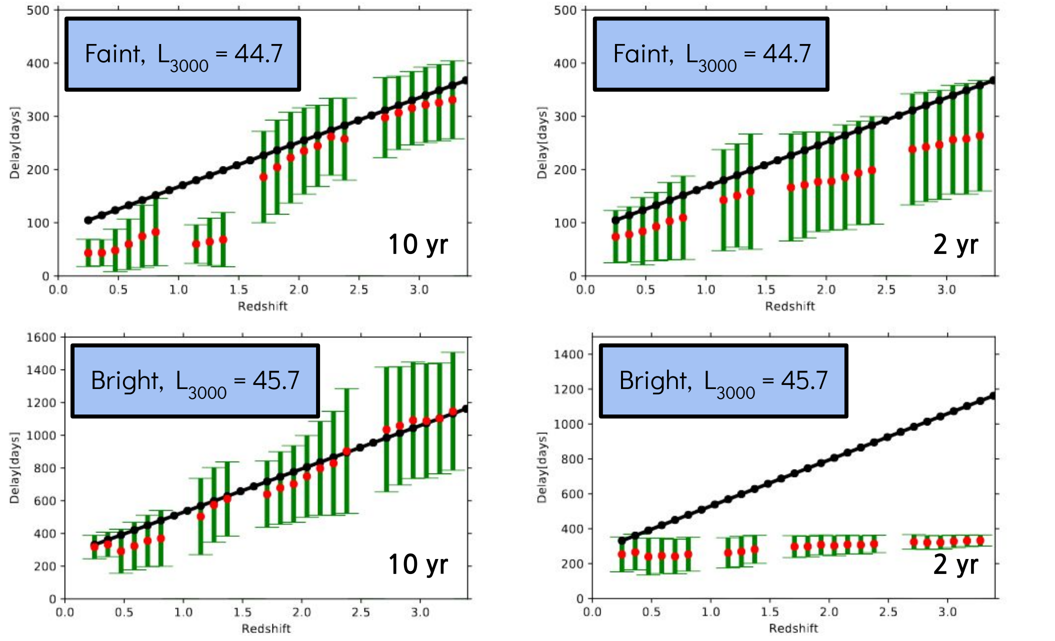

Fig. 6. The adopted and recovered time delay as a function of redshift for faint AGN ($\log L_{3000}$ = 44.7 erg s^{-1}, upper panel) and for bright AGN ($\log L_{3000}$ = 45.7 erg s^{-1}, lower panel) from 10 years of observations in the DDF. Other parameters have standard values given in Table 1.

Fig. 7. The adopted and recovered time delay as a function of redshift for faint AGN ($\log L_{3000}$ = 44.7 erg s^{-1}, upper panel) and for bright AGN ($\log L_{3000}$ = 45.7 erg s^{-1}, lower panel) from 2 years of observations in the DDF. Other parameters have standard values given in Table 1.

Table 3. The effective mean separation in the observing dates in *r* band and the redshift-averaged offset of the mean recovered time delay in comparison to the assumed time delay for bright quasars, 10 years of data

Cadence	formal name	effective separation [days]	offset in delay [%]
S1-MS	baseline_v2.0_10yrs	13.7	11.7
S4-DDF	ddf_old_rot_slf0.35_v2.1_10yrs	5.0	13
S5-DDF	ddf_quad_slf0.35_v2.1_10yrs	2.7	10
S6-DDF	ddf_quad_subfilter_slf0.35_v2.1_10yrs	3.3	10
S7-DDF	ddf_season_length_slf0.20_v2.1_10yrs	5.9	10
S8-DDF	ddf_season_length_slf0.35_v2.1_10yrs	4.7	11
S2-DDF-equal	-	1.0	11.1

Dual purpose deliverable software

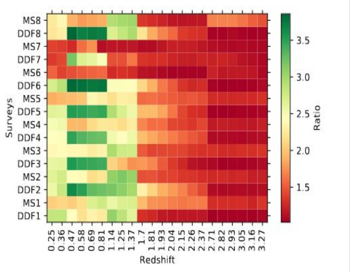

Faint, L_{3000} = 44.7

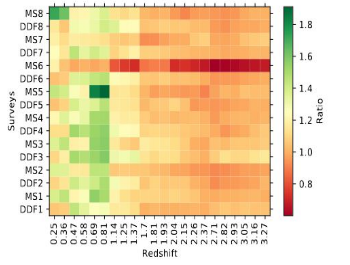

Bright, L_{3000} = 45.7

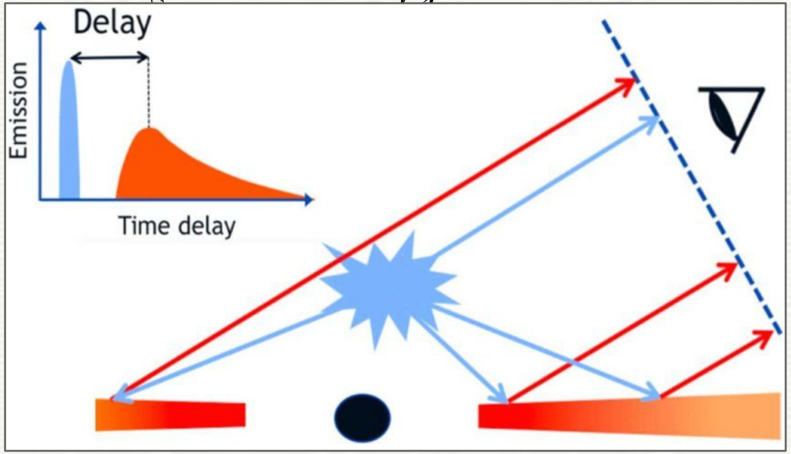

Courtesy: Phil Uttley

$$\tau = \tau_0 \left[(\lambda/\lambda_0)^{\beta} - 1 \right]$$

β ~ 1, much shallower

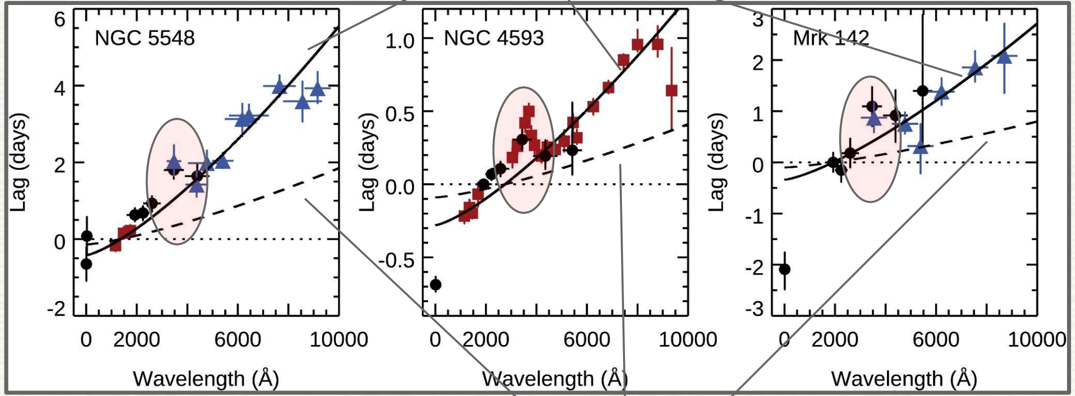

Cackett et al. (2021)

Standard Accretion disk predictions
$\beta = 4/3$

$\tau_0^{predicted} \sim 2\text{-}3\ \tau_0^{standard}{}_{disk}$

accretion disk size problem

Accretion disk continuum lags modelling and predictions

LSST White Paper (Brandt et al. 2019)

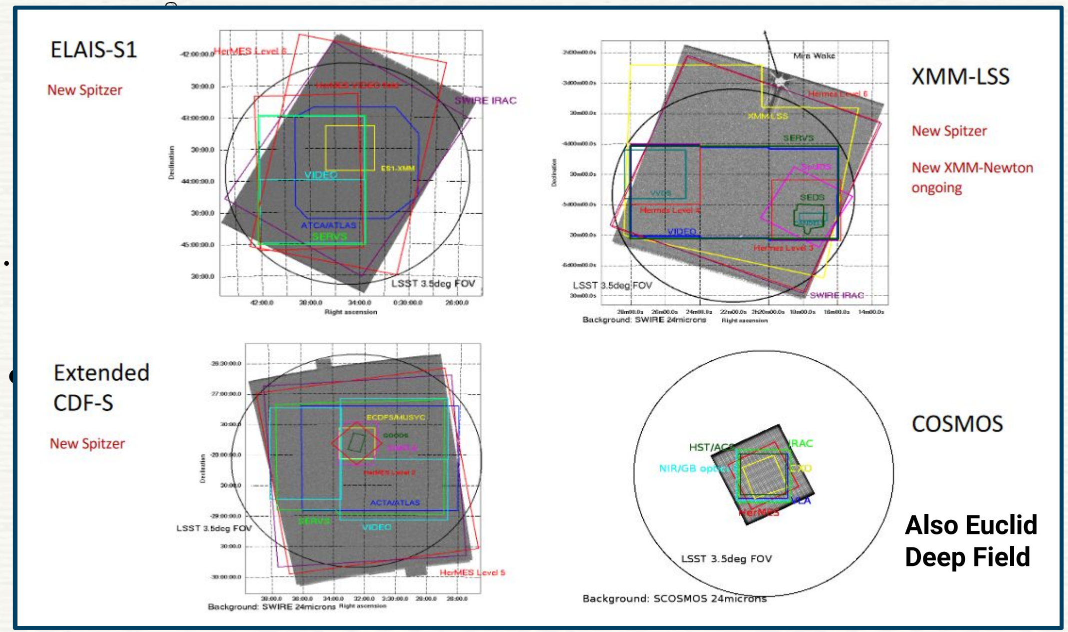

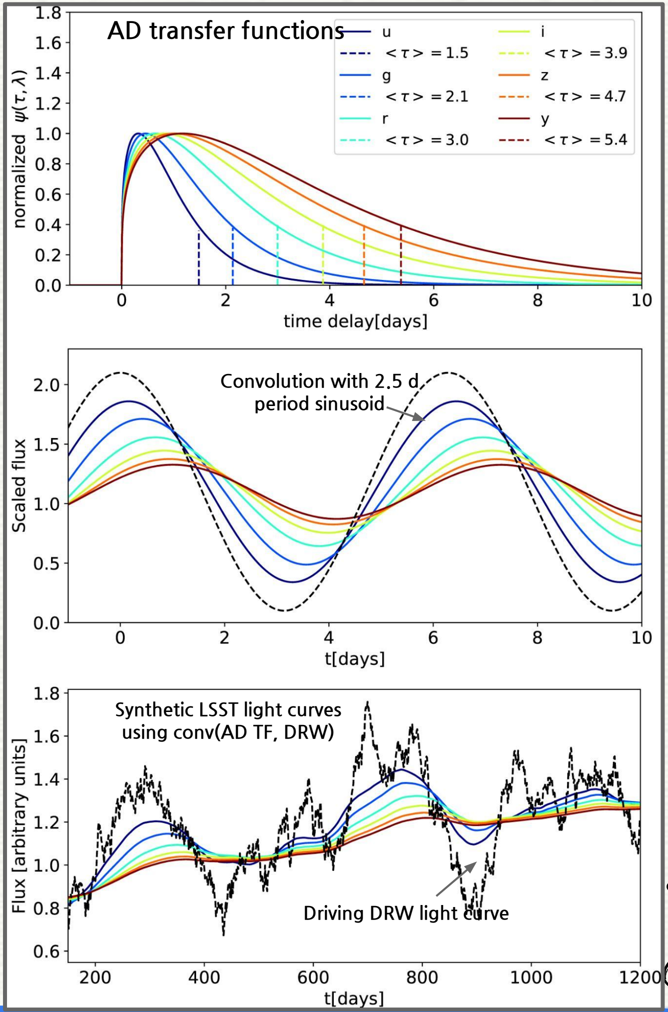

Accretion disk continuum lags modelling and predictions

- More data, more sources to verify
- Accounting for the various contaminants

Kovacevic et al. (incl. Panda), 2022

Aka Diffused continuum emission (DCE)

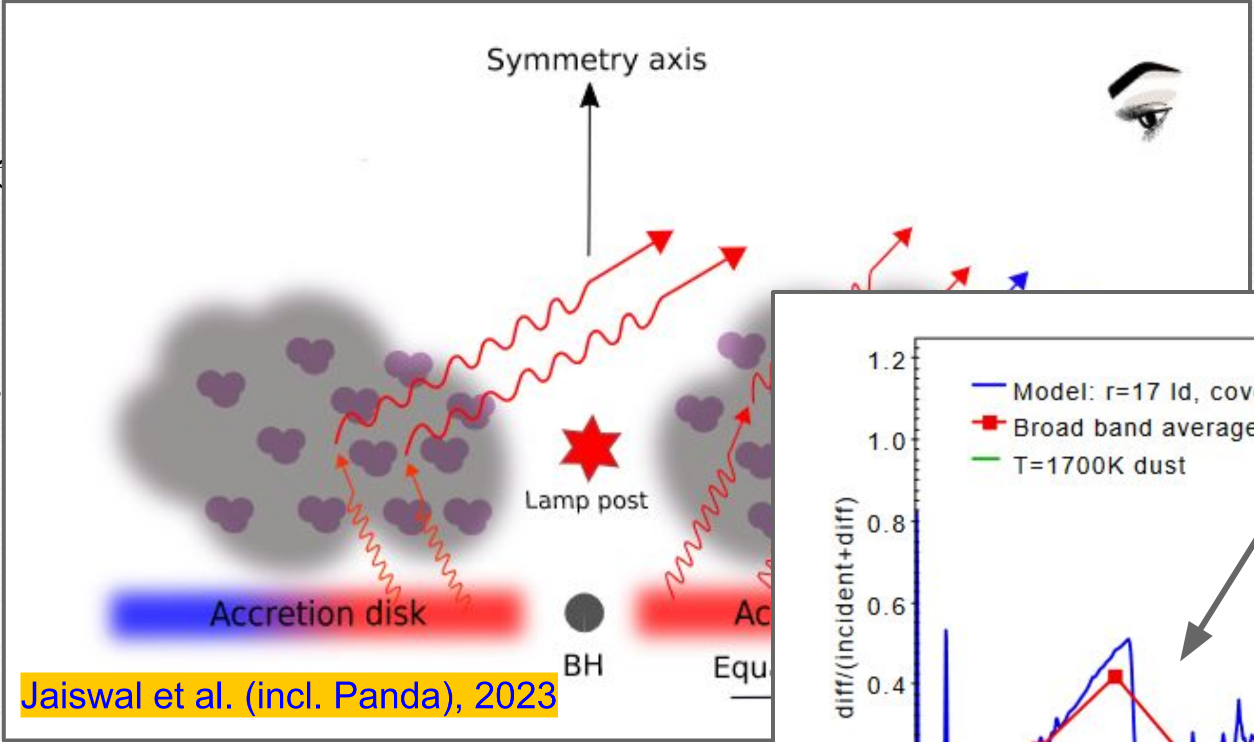

Jaiswal et al. (incl. Panda), 2023

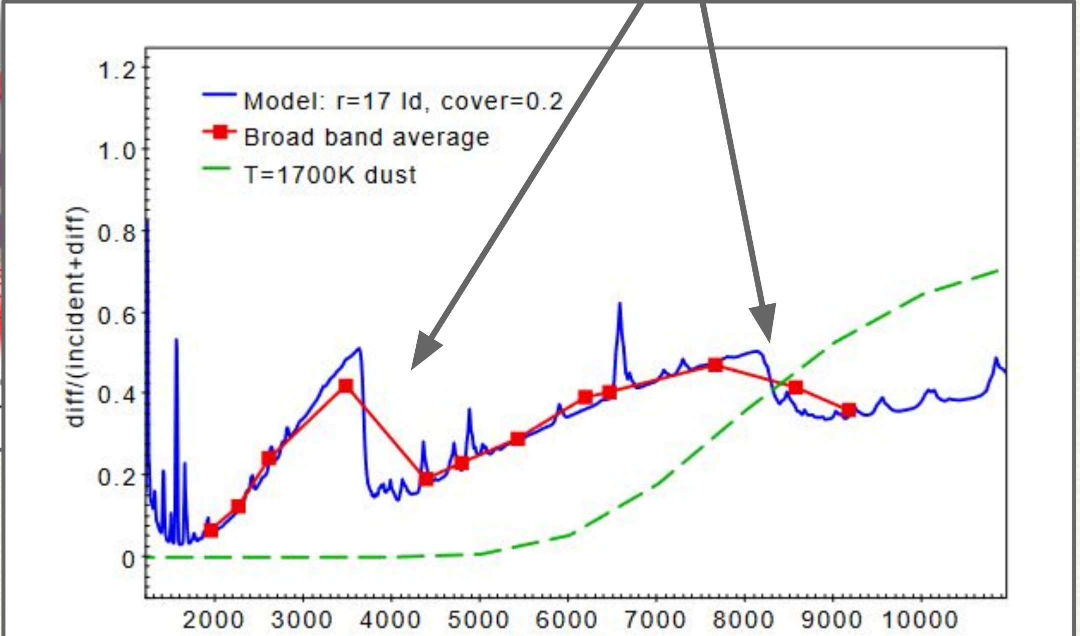

Netzer (2022)

BLR scattering
Is also important!

Pozo-Nuñez et al. (incl. Panda), 2023

AD Predictions for LSST: BLR contribution & time-sampling

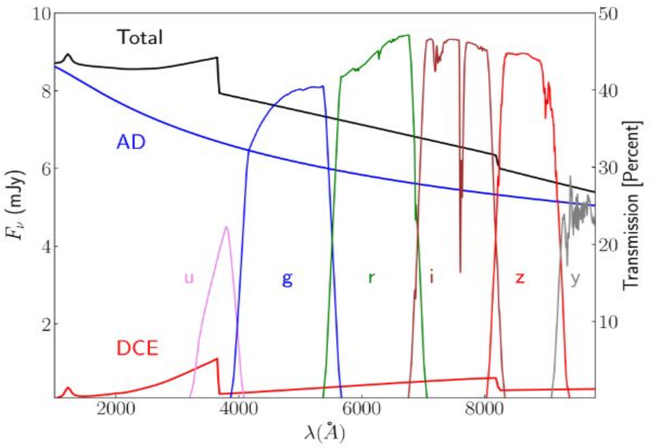

Figure 4. DCE and AD models for an arbitrary quasar obtained with the same model parameters as shown in Figure A1. The LSST transmission curves (*ugrizy*) are convolved with the quantum efficiency of the CCD camera and denoted by colored solid lines.

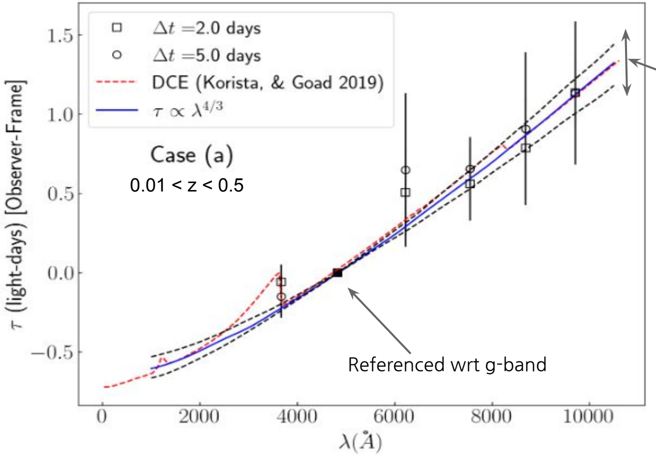

Figure 6. Same as Figure 5, but for Case(a) and an AD time delay spectrum recovered from observations with variable DCE from the BLR (red dotted line). The results are shown for a time sampling $\Delta t = 2$ days (filled squares).

The dotted lines show the delay spectrum obtained for a black hole mass with 30% uncertainty.

A minimum signal-to-noise ratio (S/N) of 100 with a BLR emission line contribution of less than 10% in the bandpasses can lead to recovery of the time delays with 5 and 10% accuracy for a time sampling of 2 and 5 days, respectively, and for quasars at 1.5 < z < 2.0

An accuracy of 10 to 20% can be achieved for quasars at z < 1.5 only if the contribution of the BLR emission lines is less than 5%.

Increasing the S/N does not improve the results significantly. Increased time sampling and reduced BLR emission line contamination is the solution to improve time delay accuracy.

02

NARROW LINE REGION (NLR)

Optical+NIR spectroscopy

Radiative transfer modelling

Coronal lines as BH mass tracers

A novel method of BH mass scaling relation using coronal lines

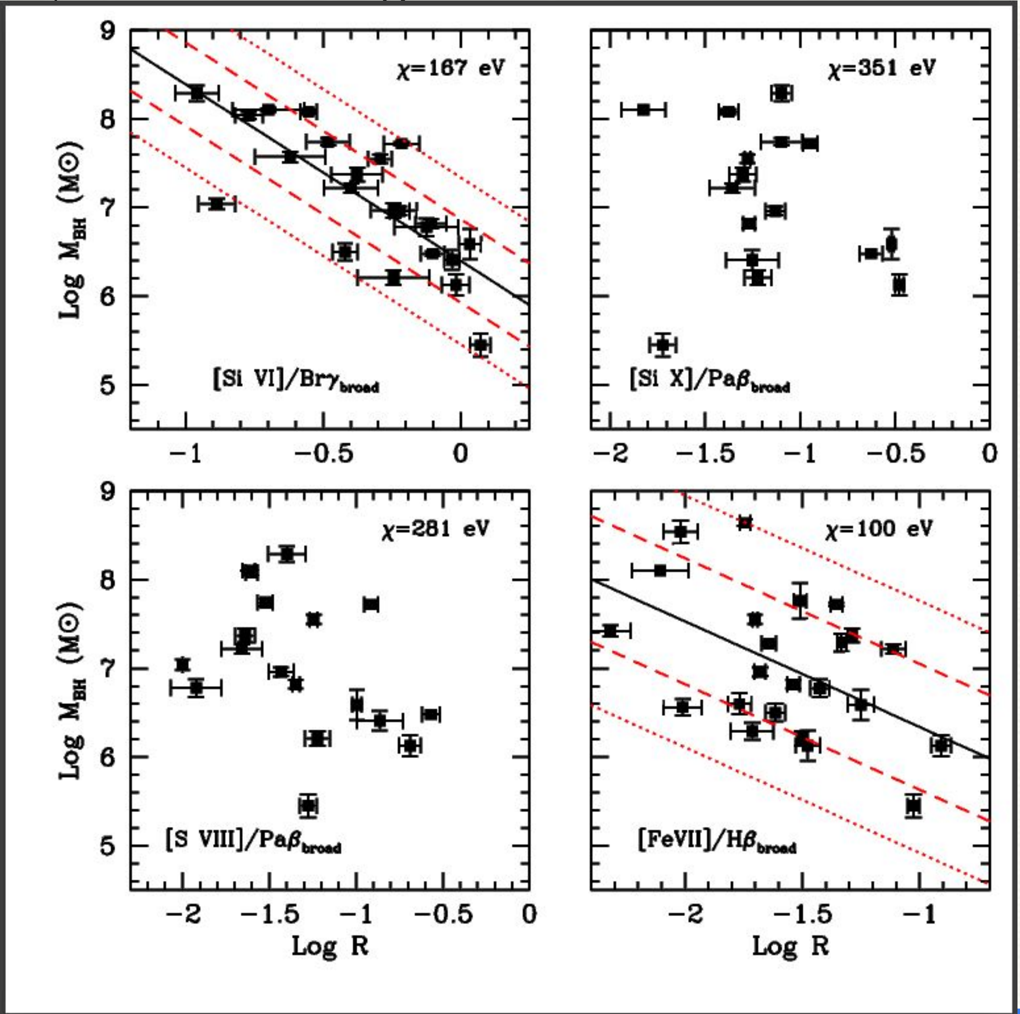

- The 31 AGNs selected in this work have BH masses determined by reverberation mapping (hence, only Type-1 AGNs) and single epoch optical and/or near-IR spectra with accurate CL measurements.

- The CL used are
    - **[Fe VII]λ6087Å** in the optical, and
    - **[S VIII]λ0.991μm**, **[Si X]λ1.432μm** and **[Si VI]λ1.964μm** in the near-IR.
    - They are among the strongest CLs in AGN (Lamperti et al. 2017), and span a wide IP range, **100 - 351 eV**.

Prieto, Rodriguez-Ardila, Panda & Marinello (2022)

Optical Spectroscopy

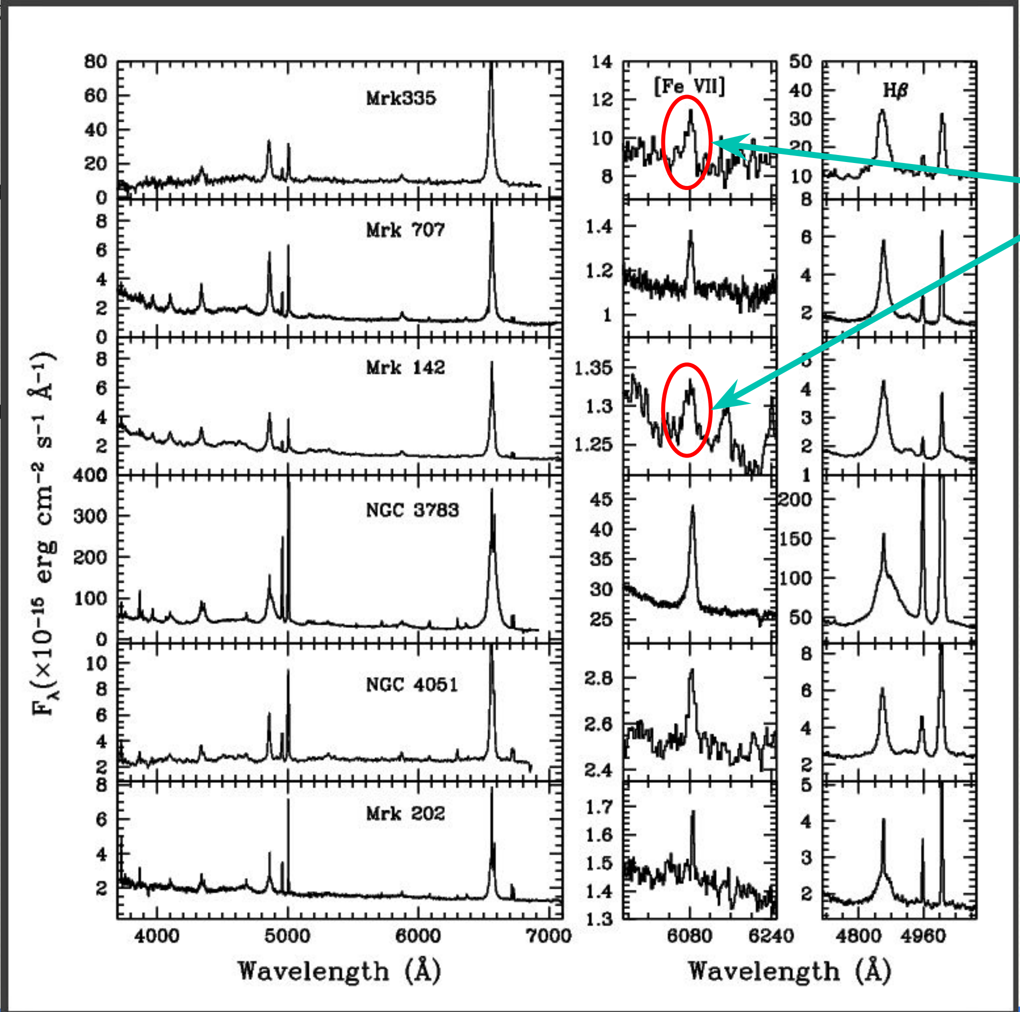

Blue-ward asymmetry → Outflows!
indication of "strong" AGN accretion

- Optical spectra were obtained either using archival database, primarily from the Sloan Digital Sky Survey (SDSS) DR7.
- For a subset of sources observed at higher redshifts, Hubble Space Telescope's FOS archival spectra were used.
- Spectra were also obtained from ground-based observatories, e.g. **2.15m CASLEO** (Argentina) and the **4.1m SOAR-Goodman** (Chile).

Prieto, Rodriguez-Ardila, Panda & Marinello (2022)

Near-Infrared (NIR) Spectroscopy

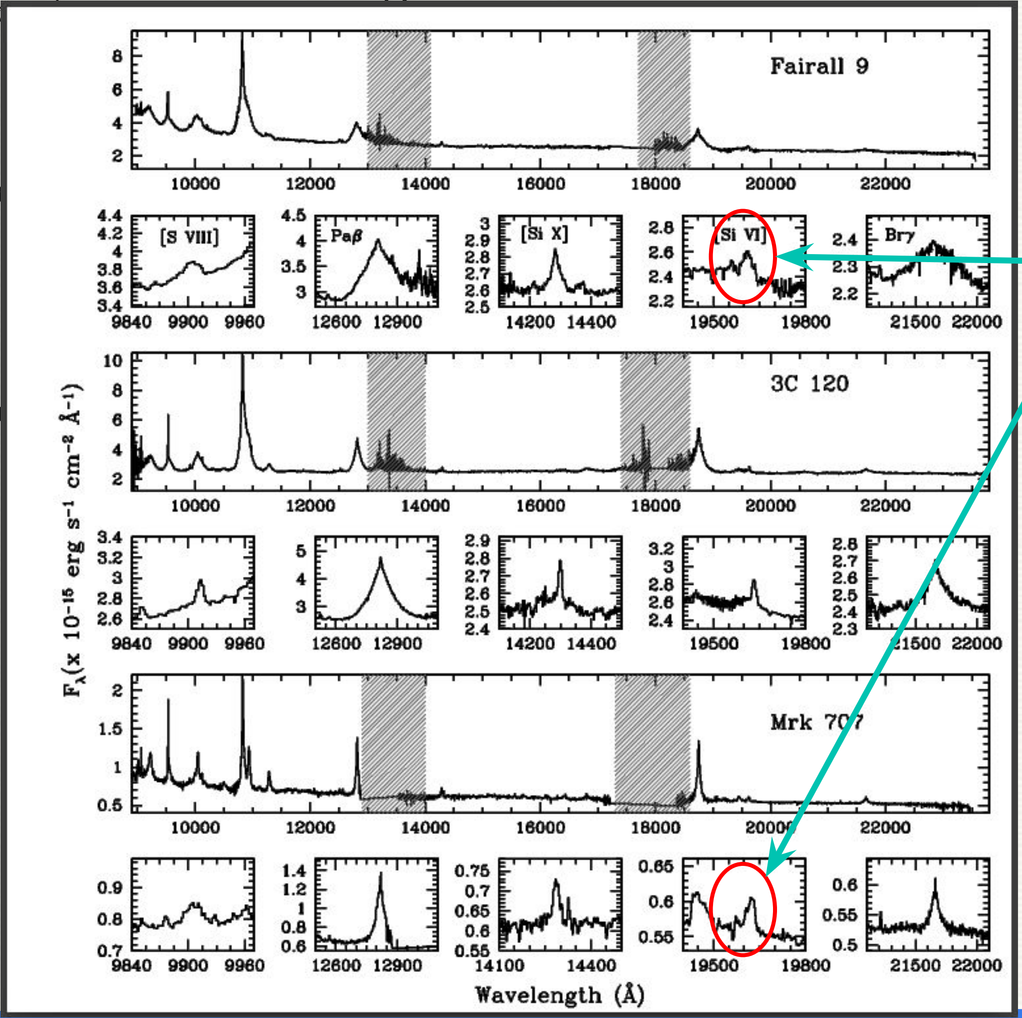

Blue-ward asymmetry → Outflows!
indication of "strong" AGN accretion

- Quasi-simultaneous NIR spectra of a few sources in our sample were taken using the **8m GEMINI-North GNIRS** (Hawaii) and the **4.1m Blanco/SOAR ARCOiRIS** (Chile).
- The NIR spectra for the remaining sources were extracted from Riffel et al. (2006).
- Standard IRAF spectral reduction, calibration and fitting techniques were employed to obtain the CL and corresponding H^+ fluxes.

Prieto, Rodriguez-Ardila, Panda & Marinello (2022)

A novel method of BH mass scaling relation using coronal lines

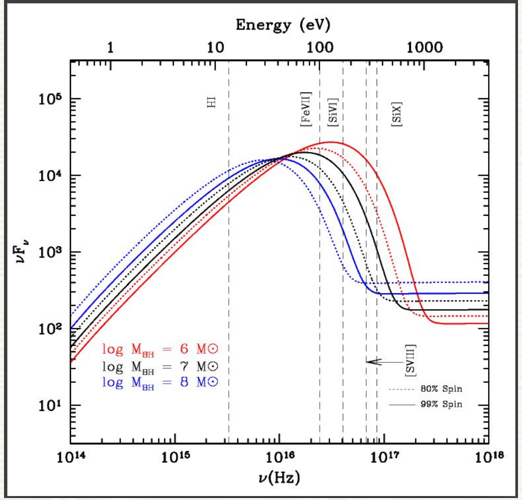

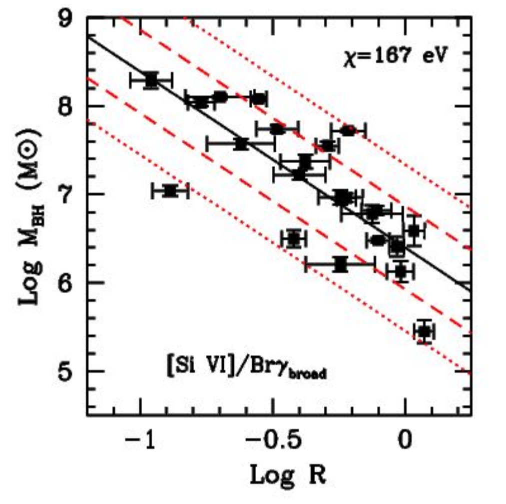

Detailed AGN/NLR parameter testing, influence on the SED shapes, BH spins

Just going to get better with the up and coming JWST data

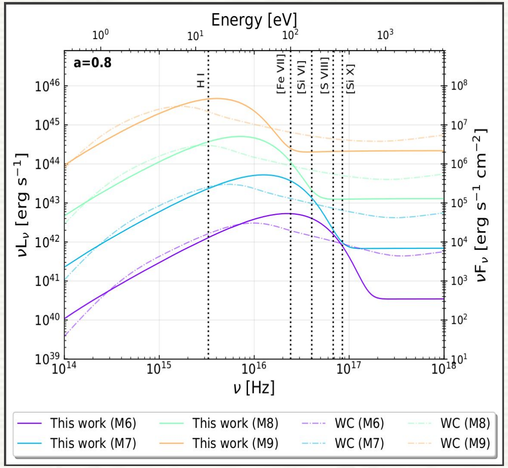

- We normalize the CL fluxes to the closest H^+ broad emission.
- Best-fit linear regression is obtained for [Si VI]/Brγ

$$\log M_{\mathrm{BH}} = (6.40 \pm 0.17) - (1.99 \pm 0.37) \times \log \left(\frac{[\mathrm{Si\ VI}]}{\mathrm{Br}\gamma_{\mathrm{broad}}} \right)$$

- with a 1σ dispersion of 0.47 dex. (0.38 dex with 15+ new AGNs), comparable with the scatter in the M-σ relation for sources with direct dynamical masses (0.44 dex).

Prieto, Rodriguez-Ardila, Panda & Marinello (2022)

U et al. (2022)

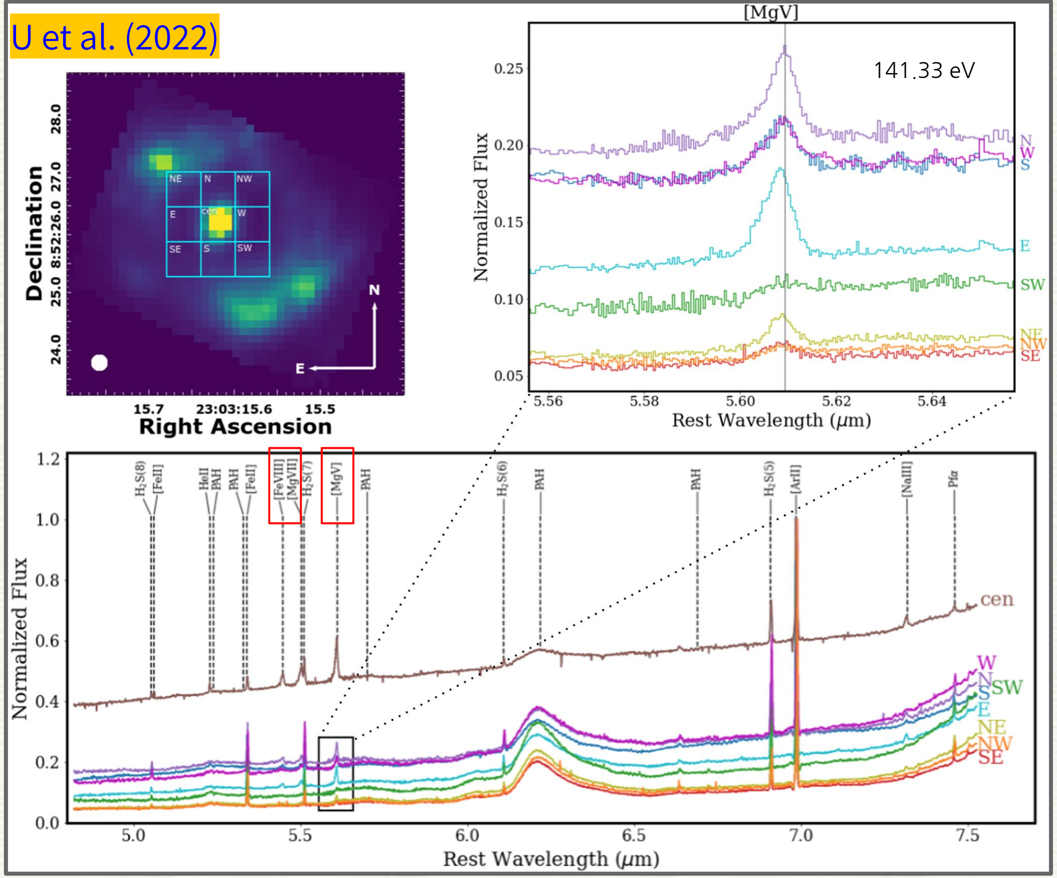

GOALS-JWST: Resolving the Circumnuclear Gas Dynamics in NGC 7469 in the Mid-infrared

Molecular and ionized gas distributions and kinematics at a **resolution of ~100 pc (4.9–7.6 μm region)**

A novel method of BH mass scaling relation using coronal lines

- We normalize the CL fluxes to the closest H^+ broad emission.
- Best-fit linear regression is obtained for [Si VI]/Brγ

$$\log M_{\rm BH} = (6.40 \pm 0.17) - (1.99 \pm 0.37) \times \log \left(\frac{[\mathrm{Si\,VI}]}{\mathrm{Br}\gamma_{\rm broad}} \right)$$

- with a 1σ dispersion of 0.47 dex., comparable with the scatter in the M-σ relation for sources with direct dynamical masses (0.44 dex).

Prieto, Rodriguez-Ardila, Panda & Marinello (2022)

03

AGNS FOR COSMOLOGY

Radius-Luminosity Relation(s)

Nuances, systematics, standardizability of these R-L relations

Our slim disk models realize why NLS1s are high accreting sources with shorter BLR time-lags → deviates from the classical R-L relation

Reconcile by correcting for Fe⁺ strength (Du & Wang 2019; Panda 2022)

Huang et al. (2019)

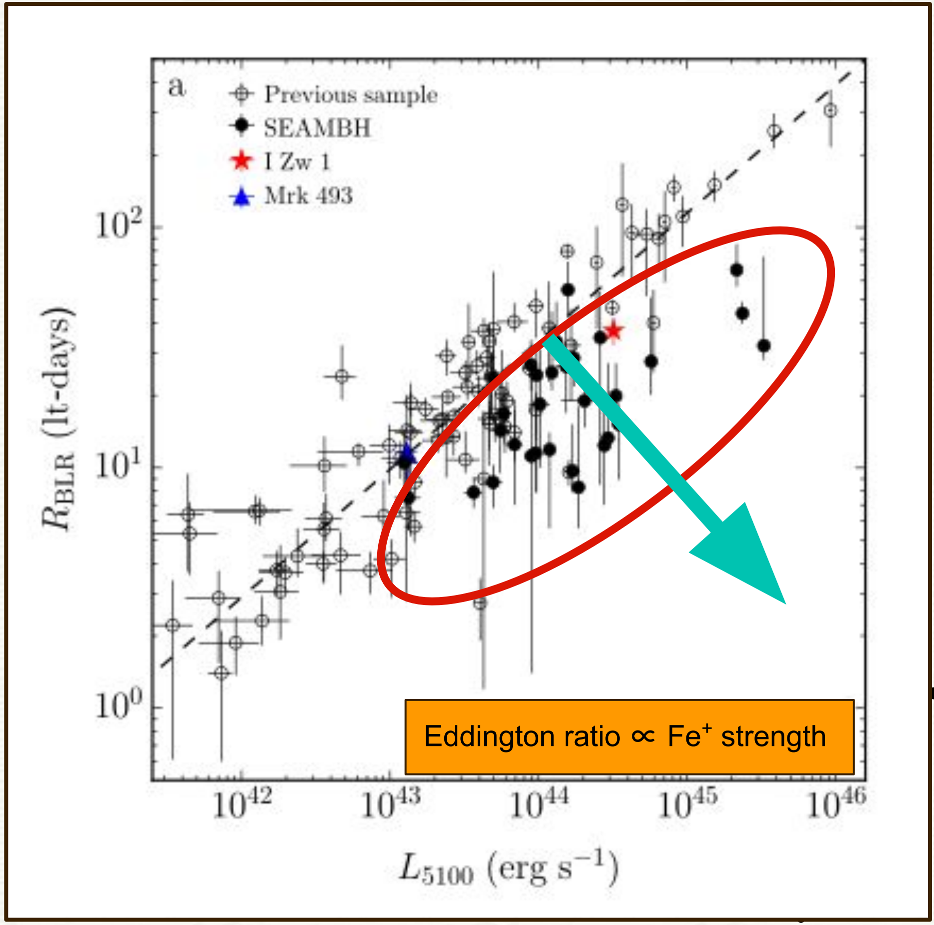

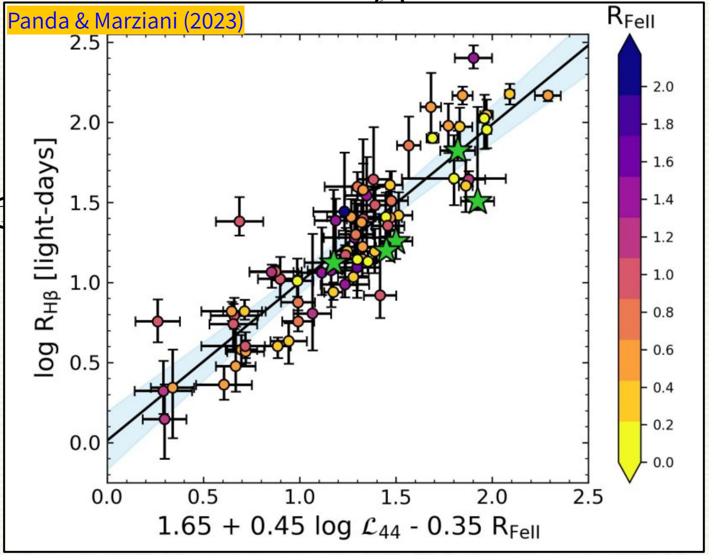

$$\log\left(\frac{R_{BLR}}{1\ \text{light}-\text{day}}\right) = \kappa + \alpha \log\left(\frac{L_{5100}}{10^{44}\ \text{erg s}^{-1}}\right) + \gamma R_{FeII}$$

$$\begin{gathered} \textit{Reverberation-mapping} \\ + \\ \textit{single-epoch spectroscopy} \end{gathered}$$

$$D_L = \sqrt{L_{5100}/4\pi F} \propto \frac{c\tau}{\sqrt{4\pi F}}$$

Why do we study these sources?

Why are the NLS1s interesting?

What is the ultimate goal?

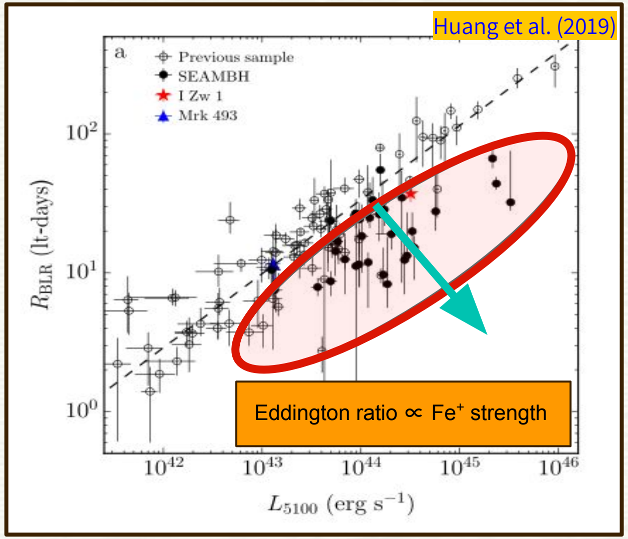

Quasars as "standardizable" candles i.e., reliable distance indicators

Local Universe
Quasars
Early Universe

Panda & Marziani (2023)

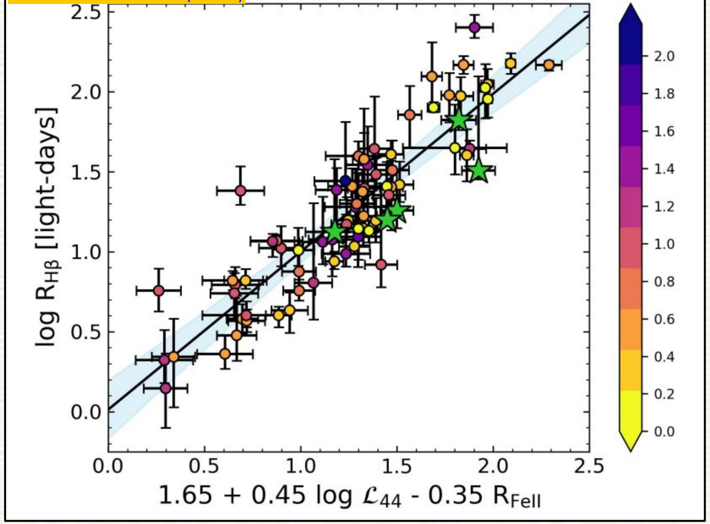

$$\log\left(\frac{R_{BLR}}{1\ \mathrm{light-day}}\right) = \kappa + \alpha \log\left(\frac{L_{5100}}{10^{44}\ \mathrm{erg\ s^{-1}}}\right) + \gamma R_{FeII}$$

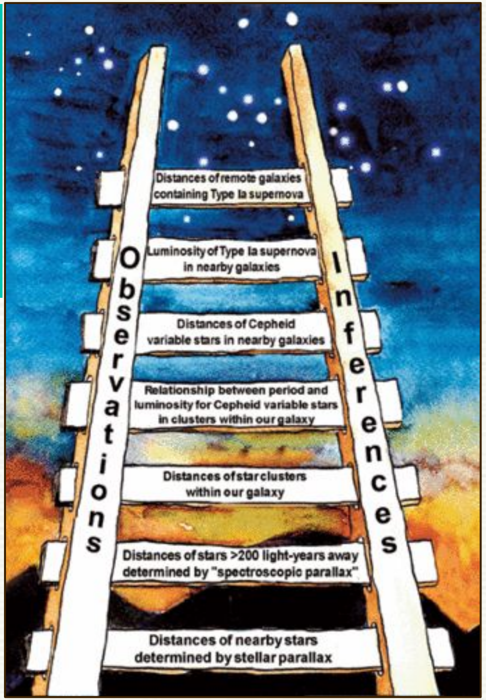

Reverberation – mapping
+
single – epoch spectroscopy

$$D_L = \sqrt{L_{5100}/4\pi F} \propto \frac{c\tau}{\sqrt{4\pi F}}$$

Panda & Marziani (2023)

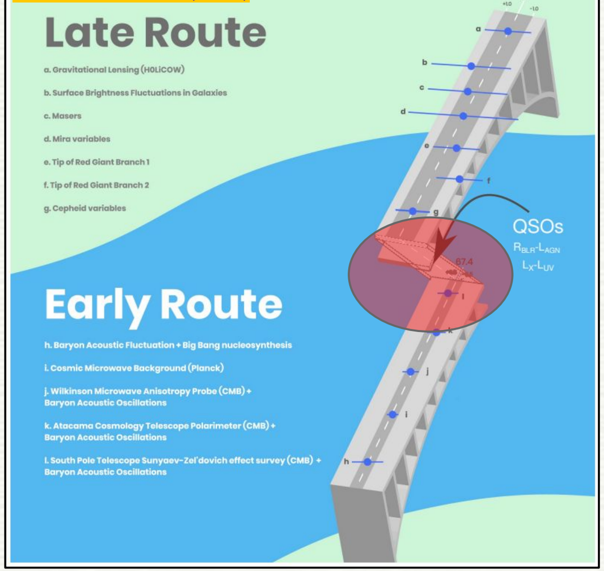

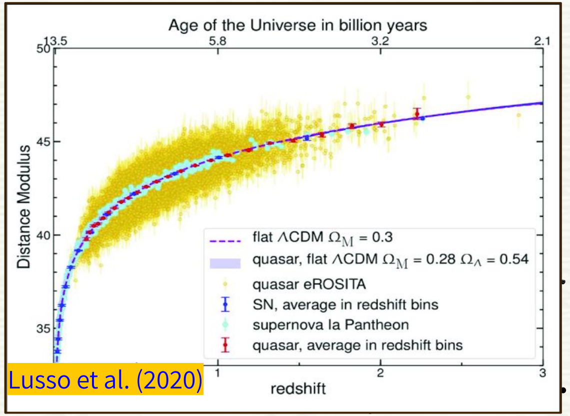

Lusso et al. (2020)

Frontiers in Astronomy and Spa... > Extragalactic Astronomy > Research Topics > Broad-Band Spectral Energy Dis...

Broad-Band Spectral Energy Distributions in AGNs - Advances and the Future

34 Total Downloads | 1,093 Views | Participate in this topic → | Submit →

Topic Editors

Swayamtrupta Panda
spanda@lna.br
Laboratório Nacional de Astrofísica
Itajubá, Brazil

Paola Marziani
paola.marziani@oapd.inaf.it
Osservatorio Astronomico di Padova (INAF)
Padua, Italy

Alberto Rodriguez-Ardila
aardila@lna.br
Laboratório Nacional de Astrofísica
Itajubá, Brazil

Preeti Kharb
kharb@ncra.tifr.res.in
Nation Centre for Radio Astrophysics, Savitribai Phule Pune University
Pune, India

frontiers

Frontiers in Astronomy and Space Sciences

4.055 Impact Factor | 4.1 CiteScore | 3,525 Citations

Manuscript Submission Deadline 30 November 2023

Email: spanda@lna.br

Thank you for your attention!

Summary

- The **diversity of active galaxies** can be understood in parts by uncovering the **physical conditions** of the gas-rich media in the vicinity of their central supermassive black holes and as a function of **fundamental BH parameters**.
- AGN variability is a fundamental property, showing distinct signatures from sub-parsecs to tens of parsecs and over wide timescales → helps constrain the R-L relation.
- BH mass tracer using coronal lines - a new, reliable scaling relation supported by photoionization
- Future is bright and data-driven - the new observatories are well-suited to discover, and utilize AGNs across wide redshifts and use them as probes for cosmology.